

Indexed by

Scopus®

MATHEMATICAL MODELLING OF HIGH-INTENSITY HEAT FLUX ON THE ELEMENTS OF HEAT-SHIELDING COMPOSITE MATERIALS OF A SPACECRAFT**Polina F. Pronina**

Moscow Aviation Institute
(National Research University),
Department of Managing
Exploitation of Space-Rocket
Systems,
Moscow, Russian Federation

Ying Sun

Hangzhou Xiaoshan
Technician College,
Department of Mechanical
Engineering,
Hangzhou, People's Republic
of China

Olga V. Tushavina

Moscow Aviation Institute
(National Research University),
Department of Managing
Exploitation of Space-Rocket
Systems,
Moscow, Russian Federation



Key words: : buckling-restrained braced frame, composite, concrete, steel, lateral displacement, base shear, energy dissipation, dynamic analysis

doi:10.5937/jaes0-28086

**Cite article:**

Pronina, F. P., Sun, Y., & Tushavina, V. O. [2020]. Mathematical modelling of high-intensity heat flux on the elements of heat-shielding composite materials of a spacecraft. *Journal of Applied Engineer-ing Science*, 18(4), 693 - 698.

Online access of full paper is available at: www.engineeringscience.rs/browse-issues

MATHEMATICAL MODELLING OF HIGH-INTENSITY HEAT FLUX ON THE ELEMENTS OF HEAT-SHIELDING COMPOSITE MATERIALS OF A SPACECRAFT

Polina F. Pronina¹, Ying Sun^{2*}, Olga V. Tushavina¹

¹Moscow Aviation Institute (National Research University), Department of Managing Exploitation of Space-Rocket Systems, Moscow, Russian Federation

²Hangzhou Xiaoshan Technician College, Department of Mechanical Engineering, Hangzhou, People's Republic of China

The main purpose of this paper is to evaluate the structural response of composite steel-concrete eccentrically buckling-restrained braced frames (BRBFs). The finite element (FE) software ABAQUS is employed to nonlinearly analyse the BRBFs. Comparing the modelling and experimental test results validates the FE modelling method of the BRBF. Three different strong earthquake records of Tabas, Northridge, and Chi-Chi are selected for the nonlinear dynamic analyses. A BRBF is then designed having a shear link. Afterwards, the designed BRBF is analysed under the selected earthquake records using the validated modelling method. The lateral displacements, base shears, and energy dissipations of the frame and shear link rotations are achieved from the analyses of the BRBF. The results are compared and discussed. The obtained BRBF results are also compared with their corresponding steel eccentrically braced frame (EBF) results. It is concluded that the BRBF can generally accomplish the improved structural response compared with the EBF under the earthquake records. Meanwhile, the BRBF has larger base shear capacity than the EBF. Moreover, the BRBF dissipates more energy than the EBF.

Key words: buckling-restrained braced frame, composite, concrete, steel, lateral displacement, base shear, energy dissipation, dynamic analysis

INTRODUCTION

During the operation of a reusable space system, about twenty external factors act on its heat-shielding elements [1-2]. These include: intense aerodynamic heating with a different chemical composition of the atmosphere, high and low temperatures caused by gas dynamics of supersonic flows, cosmic radiation, solar radiation, etc. As a rule, heat-shielding structural elements are multifunctional composite layered materials with complex properties, saturated with various binding substances. Besides, the outboard edges and some inside surfaces of these elements have various heat-shielding coatings, which significantly increase its service life [3-5].

During the operation of space-based technology, the heat-shielding coating is directly affected by all of the previously listed factors [6-8], however, the most dangerous from the standpoint of aging and destruction are high-intensity energy flows and high temperatures. Therefore, in this paper, first of all, the effect of high-intensity heat fluxes of energy on the surface of heat-shielding composite materials is considered.

Composite materials are widely used in aviation and rocket and space technology as structural and heat-shielding materials due to their unique properties resulting from their manufacturing technology. The matrix of fine-fibre fillers is saturated with binding substances that are easily decomposed at moderate temperatures [9-11]. When such materials are used as heat shielding materials at

hypersonic flight speeds, heat fluxes from high-temperature boundary layers are absorbed [12-14]. The heat and mass transfer process is presented in Fig. 1.

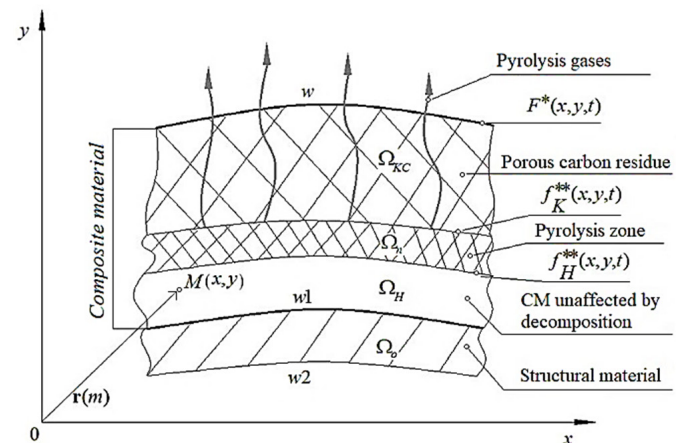


Figure 1: Modeling of heat and mass transfer in anisotropic composite materials under high-temperature loading

From Figure 1 it follows that at temperatures up to ~600K the heat-shielding material operates due to its thermo-physical characteristics, namely, the volumetric heat capacity and heat transfer inside the material due to its thermal conductivity. Above this temperature, decomposition of the binding agent begins under the action of endothermic chemical reactions with the formation of gaseous decomposition products and a porous residue consisting of filler fibers and carbon residue from the decomposition of

the binding substance [15, 16]. Due to the decomposition of the binding substance the decomposition area, limited by the coordinates of the beginning and end of decomposition, becomes very thin and separates the material unaffected by decomposition and the porous residue in which there is no trace of decomposition.

Further, through the porous residue, under the action of a pressure gradient between the decomposition area, where the pressure due to the low filtration rate of the pyrolysis gases is considered the stagnation pressure, and the outer boundary, where the pressure is equal to the ambient pressure, the pyrolysis gases are filtered, absorbing thermal energy due to convection. At the same time, to implement the filtration process, the stagnation pressure must exceed the ambient pressure by the value of the hydraulic resistance of the porous residue [17-19]. In this case, pyrolysis gases are blown into the high-temperature boundary layer, pushing it away from the outer boundary and decreasing its temperature, which entails a decrease in convective heat fluxes to the outer boundary. When the porous residue reaches the ablation temperature, the mass removal of carbon residue of the composite material begins at the outer boundary due to physical and chemical transformations.

PHYSICAL AND MATHEMATICAL MODEL OF HEAT AND MASS TRANSFER IN HEAT-SHIELDING COMPOSITE MATERIALS UNDER HIGH-TEMPERATURE LOADING

Let us consider the effect of a high-intensity heat flux of energy on a structural element of a modern flying vehicles (FVs), consisting of a composite material (Fig. 2).

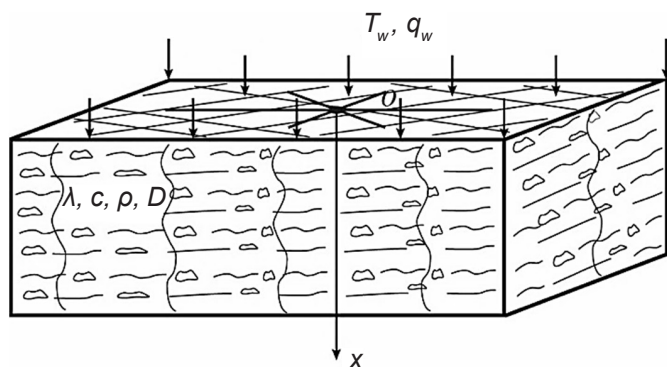


Figure 2: Diagram of loading on aircraft structural element

When developing a mathematical model of heat and mass transfer, preliminary assumptions must be made that limit its applicability and the laws of decomposition of adhesive and nonlinear filtration of pyrolysis gases through a porous residue must be formulated. To study the process of heat and mass transfer, we will formulate assumptions that allow, in the first approximation, to analytically evaluate the main parameters of the process.

1. For the problem under consideration, the computational space is assumed to be two-dimensional in spatial variables with an outer boundary w described

by an implicit function $F^*(x,y,t)=0$, which can be non-stationary under the action of mass carryover when the temperature of the outer surface exceeds the temperature of carryover masses.

2. A structural element made of composite materials (CM) is exposed to a high-intensity flow of thermal energy (Fig. 2), the computational space of which is assumed to be one-dimensional (x -axis).
3. Ω_n – the pyrolysis zone is limited by unsteady moving surfaces of the beginning $f_n^{**}(x,y,t)$ and the end $f_k^{**}(x,y,t)$ the binding substance decomposition with the formation of a gas component and a porous residue occurs.
4. Between the porous frame and pyrolysis gases, thermodynamic equilibrium is established at each point of the porous region bounded by the surfaces $f_k^{**}(x,y,t)$ and $F^*(x,y,t)$, where convective-conductive heat transfer occurs with the account for non-isothermal multidimensional filtration of pyrolysis gases.
5. It is assumed that during the filtration of pyrolysis gases, the pressure in the adhesive decomposition zone is considered as the stagnation pressure since the filtration rate there is practically zero.
6. Injection of pyrolysis gases into the gas-dynamic boundary layer is taken into account by a decrease in gas-dynamic heat fluxes depending on the injection parameter, which is the product of the density of the injected gases and the filtration rate at the outer boundary $F^*(x,y,t)$.

Taking into account the accepted assumptions, the mathematical model of unsteady heat and mass transfer in the two-dimensional region of CM at high temperatures includes the following relations:

- Balance of convective-conductive and radiant heat fluxes and heat fluxes absorbed due to mass entrainment at the boundary w in contact with the high-temperature gas-dynamic boundary layer:

$$\left(\frac{\alpha}{c_p}\right)_w (I_b - I_w) - \lambda grad T|_w - \epsilon_w \cdot \sigma \cdot T_w^4 - (P \cdot c_p \cdot \rho \cdot V)_g \cdot T_w = \dot{m} \cdot Q^*(I_e) \cdot \eta (T_w - T^*), \quad (1)$$

$$(x, y) \in w, t > 0$$

where $\left(\frac{\alpha}{c_p}\right)_w$ coefficient of heat transfer from the boundary layer, referred to the heat capacity of the gas-dynamic flow at the wall temperature, taking into account the injection.

$$\left(\frac{\alpha}{c_p}\right)_w = \left(\frac{\alpha}{c_p}\right)_{w0} - \beta \cdot (\rho_g V_g)_w \quad (2)$$

Where β – injection parameter.

$$\beta = 0.56 \left(\frac{M_a}{M}\right)^{0.29} \cdot \left(\frac{I_w}{I_b}\right) \quad (3)$$

Where \bar{M} – weighted-average molar mass of pyrolysis gases mixture; M_a – molar mass of air; I_b – effective enthalpy of the boundary layer.

$$I_b = c_{pn} \cdot T_n + \frac{V_n^2}{2} \quad (4)$$

c_{pn} , T_n , V_n – respectively, the heat capacity, temperature, speed of the oncoming gas-dynamic flow; I_w – enthalpy of the gas at the wall temperature, $I_w = \int_0^{T_w} c_p(T) dT$; ϵ_w , σ , Q^* , T – respectively, the degree of surface emissivity, Stefan-Boltzmann constant, effective enthalpy of CM, temperature of CM mass carryover; Λ – thermal conductivity tensor of the CM, \dot{m} – mass velocity of mass carryover, $\dot{m} = \rho \cdot \dot{n}^*$ where \dot{n}^* – linear velocity of mass loss in the direction normal to the surface $F^*(x,y,t)$; $\eta(z)$ – the Heaviside step function.

- Heat transfer equation in structural material:

$$c_0(T)\rho_0 \frac{\partial T}{\partial t} = \text{div}(\Lambda_0 \text{grad}T), (x,y) \in \Omega_0, t > 0 \quad (5)$$

where Λ_0 – structural material thermal conductivity tensor.

- Mathematical model of coupled thermoelasticity for determination of the stress-strain state of a heat-shielding composite element (Fig. 2) [20-22]:

$$\frac{\partial^2 u}{\partial \tau^2} = \frac{\partial^2 u}{\partial x^2} - b_u \frac{\partial T}{\partial x} \frac{\partial T}{\partial \tau} = k \frac{\partial^2 T}{\partial x^2} - b_T \frac{\partial^2 u}{\partial x \partial \tau} \quad (6)$$

where u, T – displacement, temperature field, concentration change, respectively; k – heat capacity coefficients, x, τ – time and coordinate; b_t – coefficients connecting the combined thermoelasticity problem.

- Initial conditions for temperature and moving boundaries:

$$T(x,y,0) = T(x,y), (x,y) \in \Omega \quad (7)$$

$$f_n^{**}(x,y,0) = \varphi(x,y), (x,y) \in f_n^{**}(x,y,0) \quad (8)$$

$$f_k^{**}(x,y,0) = \psi(x,y), (x,y) \in f_k^{**}(x,y,0) \quad (9)$$

where Ω – initial region between the boundaries w_2 and w , not subject to phase transformations.

- Continuity of heat fluxes and temperatures at the boundary $f_{w1}(x,y)$ between CM and structural material:

$$\Lambda \text{grad}T|_{f_{w1+0}} - \Lambda_0 \text{grad}T|_{f_{w1-0}} = 0, T|_{f_{w1+0}} = T|_{f_{w1-0}}, (x,y) \in w_1, t > 0 \quad (10)$$

- Balance of convective-conductive and radiant heat fluxes on the inner free boundary w_2 :

$$\alpha_{w2}(T_{b2} - T_{w2}) + \Lambda_0 \text{grad}T|_{w2} - \epsilon_{w2} \sigma T_{w2}^4 = 0 \quad (11)$$

$(x,y) \in w_2, t > 0$

- Thermal conductivity equation with allowance for filtration in the porous residue:

$$c_{bfff}(T) \cdot \rho_{bfff} \frac{\partial T}{\partial t} = \text{div}(\Lambda_{eff} \text{grad}T) - P(c_p \rho \cdot V)_g \text{grad}T, (x,y) \in \Omega_{kc}, t > t_k^{**} \quad (12)$$

where t_k^{**} – time of occurrence of the boundary $f_k^{**}(x,y,t)$.

- Energy equation in the adhesive decomposition zone with account for physicochemical transformations with thermal effect Q^{**} and filtration:

$$c_{bfff}(T) \cdot \rho_{bfff}(T) \frac{\partial T}{\partial t} = \text{div}(\Lambda_{bfff} \text{grad}T) - \dot{\rho}(x,y,t) \cdot Q^{**} - P^{**}(x,y)(c_p \rho V)_g \text{grad}T, \quad (13)$$

$(x,y) \in \Omega_n, t > t_n^{**}$

where $P^{**}(x,y)$ changes linearly in the direction normal to the boundary $f_n^{**}(x,y,t)$ from the value $P^{**}=0$ on this boundary to the value $P^{**}=P$ on the boundary $f_k^{**}(x,y,t)$ – equation of state of pyrolysis gases.

$$\rho_g = \frac{p_g \cdot \bar{M}_g}{R_g \cdot T}, (x,y) \in \Omega_{kc} t > t_k^{**} \quad (14)$$

For the coupled thermoelasticity problem (6), the standard conditions for the first initial-boundary value problem are satisfied. Further, to the given system of equations, it is necessary to add the law of changes in the CM density in the adhesive decomposition zone and the Stefan conditions on the nonstationary moving boundary of the beginning and end of the adhesive decomposition, as well as the continuity equation for filtration of pyrolysis gases and the law of nonlinear filtration of pyrolysis gases [23, 24].

The mathematical model (1-14) is complex, consisting of several mathematical models:

- heat conduction problem in anisotropic medium with heat conduction tensor Λ_0 ;
- heat and mass transfer in porous carbon residue Ω_{cb} limited by two nonstationary moving boundaries $f_k^{**}(x,y,t)$ and $F(x,y,t)$ taking into account mass carryover, filtration of pyrolysis gases, and their injection into the boundary layer, emission and tensor nature of nonlinear heat and mass transfer;
- non-isothermal multidimensional filtration of pyrolysis gases in anisotropic porous residue by determining the fields u and v of the filtration components rate and pressure of pyrolysis gases.
- problem of coupled thermoelasticity for a composite rod in the one-dimensional formulation [25].

The mathematical model is closed by the equation for determining the CM density in the pyrolysis zone and the stagnation pressure of pyrolysis gases, as well as the nonlinear law of filtration of pyrolysis gases in a porous medium.

SOLUTION OF MULTIDIMENSIONAL PROBLEMS OF HEAT AND MASS TRANSFER IN ANISOTROPIC COMPOSITE MATERIALS UNDER HIGH-TEMPERATURE LOADING

The presented mathematical model is a problem of non-linear anisotropic coupled thermoelasticity in the presence of convective-conductive and radiant types of heat transfer at free boundaries. In the problems of heat and mass transfer, due to the significant nonlinearity of the complex problem, only implicit numerical schemes are used, as a result of which we can expect the stability of the numerical solution and its convergence to the exact one.

It should be noted that in problems of heat and mass transfer with phase transformations, the temperature distribution significantly affects the rate of phase transformations, and phase transformations, in turn, significantly change the temperature fields. As a result, in such problems, the step of numerical integration overtime should be related to the rate of phase transformations or the velocities of motion of phase transformations boundaries even when using completely implicit numerical schemes. This is confirmed by numerical experiments [26-28].

If the step of numerical integration in time is not consistent with the velocities of motion of the phase transformations boundaries, then the solution falls apart due to the fact

that, at an arbitrary step in time, the boundaries of phase transformations can move deep into the composite so the temperature field, which depends on the coordinates of these boundaries, will not be connected with the temperature field at the previous time layers [29-30]. Further, the results of numerical modelling of heat and mass transfer in anisotropic composite materials are presented based on the developed software package that implements the developed complex mathematical model [31-32]. The following input data were taken for calculations: $l_1 = 0.15m$; $l_2 = 0.05m$; $T_0(x,y) = 300K = const$; $\alpha_{wi} = 1 kBm/m^2 \cdot K$; $T_{wi} = 300K$, $i = 2,3,4$; $c^{(1)} = 1kJ/kg \cdot K$; $\rho^{(1)} = 2500 kg/m^3$; $c^{(2)} = 0.5kJ/kg \cdot K$; $\rho^{(2)} = 2000kg/m^3$; $T^* = 800K$; $Q^* = 1000kg$; $\lambda_{\xi}^{(1)} = 1kV/m \cdot K$; $\lambda_{\eta}^{(1)} = 0.5kV/m \cdot K$. Figure 3 reveals the results of calculations of a Stefan-type problem in a two-dimensional anisotropic rod with a nonstationary moving boundary of phase transformations in the form of curves $T(x,y)$ and nonstationary moving boundaries $y = y(x,t)$ $\lambda_{\xi}^{(2)} = \lambda_{\eta}^{(2)} = 1kV/m \cdot K t_{con} = 10c$, where index (2) refers to the reacted phase, and (1) – to the initial phase. In the orthotropic case $\lambda_{11} = \lambda_{\xi}$, $\lambda_{22} = \lambda_{\eta}$, if the angle φ , orienting the main axes, is equal to zero and $\lambda_{11} = \lambda_{\eta}$, $\lambda_{22} = \lambda_{\xi}$, if $\varphi = \pi/2$. It can be seen from these figures that an increase (decrease) in the λ_{11} component increases the heating and the speed of the boundary movement $y = f(x^*(t), t)$.

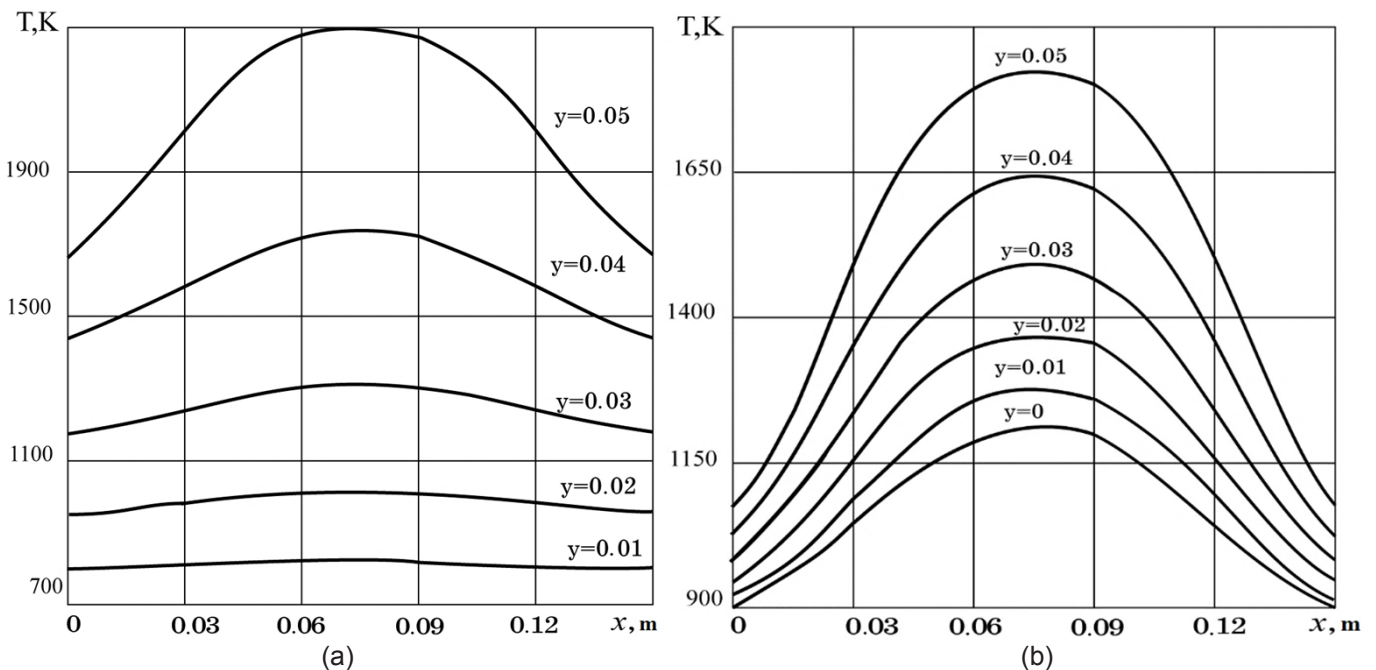


Figure 3: Temperature field at time moment $t_{con} = 10c$ (a) phase transformations for the orthotropic case $\varphi = 0$ (a) and $\varphi = \pi/2$ (b)

The heat transfer parameters and the characteristics of the thermal conductivity tensor were taken as follows: $\alpha = 5 kV/(m^2 \cdot K)$, $T_{b1} = 10^4 K$, $\lambda_{11} = 0.8 kV/(m \cdot K)$, $\lambda_{12} = 0.25 kV/(m \cdot K)$, $\lambda_{22} = 0.2 kV/(m \cdot K)$. The input data were taken as follows: in a two-dimensional anisotropic region made of composite material $\lambda_{\xi} = 0.0009 kV/(m \cdot K)$;

$\lambda_{\eta} = 0.0006 kV/(m \cdot K)$; $\lambda_{\xi ks} = 0.0012 kV/(m \cdot K)$; $\lambda_{\eta ks} = 0.0025 kV/(m \cdot K)$; $\rho_n = 1600 kg/m^3$; $\rho_k = 1250 kg/m^3$; $T^{ks} = 750 K$; $Q^{ks} = 1030 kJ/kg$; $\epsilon_1 = 0.8$; $\epsilon_2 = \epsilon_3 = \epsilon_4 = 0$; $l_1 = 0.15 m$; $l_2 = 0.05 m$; $p_{w1} = 10^5 Pa$; $P = 0.4$; $k = 10^{-14} m^2$; $M = 0.4 kg/mole$; $t_{con} = 20c$; $\tau = 0.5 c$; $T_{b1} = 4000 K$; $T_{b2} = T_{b3} = T_{b4} = 300 K$; $T_n = 300 K$.

CONCLUSIONS

The calculation results have revealed that: the stronger the thermal load, the stronger the shift of the above-mentioned maxima in the direction of deviation of the temperature field in the direction of the greater thermal conductivity; the temperature of deeper points from the border is higher than the temperature of points closer to the border. Also, it was identified that the significant asymmetry of the boundary of phase transformations and the temperature field is visible even with a small degree of anisotropy. Numerical calculations showed that the temperature field has maxima shifted from the axis of symmetry $x = l_1/2$ of the heat load in the direction of the $O\xi$ with a large thermal conductivity coefficient, and the deeper from the boundary $y = l_2$, on which the principal axis with a large thermal conductivity coefficient is also set.

ACKNOWLEDGMENTS

The work was carried out with the financial support of the state project of the Ministry of Education and Science project code FSFF-2020-0016.

REFERENCES

1. Bulychev, N.A., Rabinskiy, L.N. (2019). Surface modification of titanium dioxide nanoparticles with acrylic acid/isobutylene copolymer under ultrasonic treatment. *Periodico Tche Quimica*, vol. 16, no. 32, 338-344.
2. Astapov, A.N., Lifanov, I.P., Rabinskiy, L.N. (2019). Perspective heat-resistant coating for protection of CF/SiC composites in air plasma hypersonic flow. *High Temperature*, vol. 57, no. 5, 744-752.
3. Antufev, B.A., Egorova, O.V., Medvedskii, A.L., Rabinskiy, L.N. (2019). Dynamics of shell with destructive heat-protective coating under running load. *INCAS Bulletin*, vol. 11, 7-16.
4. Antufiev, B.A., Egorova, O.V., Orekhov, A.A., Kuznetsova, E.L. (2018). Dynamics of thin-walled structure with high elongation ratio and discrete elastic supports on the rigid surface under moving loads. *Periodico Tche Quimica*, vol. 15, no. 1, 464-470.
5. Kuznetsova, E.L., Makarenko, A.V. (2019). Mathematical model of energy efficiency of mechatronic modules and power sources for prospective mobile objects. *Periodico Tche Quimica*, vol. 16, no. 32, 529-541.
6. Kuznetsova, E.L., Rabinskiy, L.N. (2019). Numerical modeling and software for determining the static and linkage parameters of growing bodies in the process of non-stationary additive heat and mass transfer. *Periodico Tche Quimica*, vol. 16, no. 33, 472-479.
7. Rabinsky, L.N., Kuznetsova, E.L. (2019). Simulation of residual thermal stresses in high-porous fibrous silicon nitride ceramics. *Powder Metallurgy and Metal Ceramics*, vol. 57, no. 11/12, 663-669.
8. Formalev, V.F., Kolesnik, S.A., Kuznetsova, E.L. (2019). Effect of components of the thermal conductivity tensor of heat-protection material on the value of heat fluxes from the gasdynamic boundary layer. *High Temperature*, vol. 57, no. 1, 58-62.
9. Ryndin, V.V. (1980). Mathematical modeling of the process of filling an engine through an inlet manifold. *Izvestia vyssih ucebnyh zavedenij. Masinostroenie*, vol. 2, 71-75.
10. Kuznetsova, E.L., Rabinskiy, L.N. (2019). Numerical modeling and software for determining the static and linkage parameters of growing bodies in the process of non-stationary additive heat and mass transfer. *Periodico Tche Quimica*, vol. 16, no. 33, 472-479.
11. Kuznetsova, E.L., Rabinskiy, L.N. (2019). Heat transfer in nonlinear anisotropic growing bodies based on analytical solution. *Asia Life Sciences*, vol. 2, 837-846.
12. Formalev, V.F., Kolesnik, S.A. (2019). On thermal solitons during wave heat transfer in restricted areas. *High Temperature*, vol. 57, no. 4, 498-502.
13. Makarenko, A.V., Kuznetsova, E.L. (2019). Energy-efficient actuator for the control system of promising vehicles. *Russian Engineering Research*, vol. 39, no. 9, 776-779.
14. Astapov, A.N., Kuznetsova, E.L., Rabinskiy, L.N. (2019). Operating capacity of anti-oxidizing coating in hypersonic flows of air plasma. *Surface Review and Letters*, vol. 26, no. 2, article number 1850145.
15. Rabinskiy, L.N. (2019). Non-stationary problem of the plane oblique pressure wave diffraction on thin shell in the shape of parabolic cylinder. *Periodico Tche Quimica*, vol. 16, no. 32, 328-337.
16. Antufev, B.A., Egorova, O.V., Rabinskiy, L.N. (2019). Quasi-static stability of a ribbed shell interacting with moving load. *INCAS Bulletin*, vol. 11, 33-39.
17. Antufev, B.A., Egorova, O.V., Rabinskiy, L.N. (2019). Dynamics of a cylindrical shell with a collapsing elastic base under the action of a pressure wave. *INCAS Bulletin*, vol. 11, 17-24.
18. Bulychev, N.A., Rabinskiy, L.N. (2019). Ceramic nanostructures obtained by acoustoplasma technique. *Nanoscience and Technology: An International Journal*, vol. 10, no. 3, 279-286.
19. Skvortsov, A.A., Zuev, S.M., Koryachko, M.V. (2018). Contact melting of aluminum-silicon structures under conditions of thermal shock. *Key Engineering Materials*, vol. 771, 118-123.

20. Dinzhos, R.V., Lysenkov, E.A., Fialko, N.M. (2015). Influence of fabrication method and type of the filler on the thermal properties of nanocomposites based on polypropylene. *Voprosy Khimii i Khimicheskoi Tekhnologii*, vol. 5, no. 103, 56-62.
21. Formalev, V.F., Kartashov, E.M., Kolesnik, S.A. (2019). Simulation of nonequilibrium heat transfer in an anisotropic semispace under the action of a point heat source. *Journal of Engineering Physics and Thermophysics*, vol. 92, no. 6, 1537-1547.
22. Formalev, V.F., Bulychev, N.A., Kuznetsova, E.L., Kolesnik, S.A. (2019). The thermal state of a packet of cooled microrocket gas-dynamic lasers. *Technical Physics Letters*, vol. 46, no. 3, 245-248.
23. Kolesnik, S.A., Bulychev, N.A. (2020). Numerical analytic method for solving the inverse coefficient problem of heat conduction in anisotropic half-space. *Journal of Physics: Conference Series*, vol. 1474, no. 1, article number 012024.
24. Formalev, V.F., Kartashov, E.M., Kolesnik, S.A. (2020). On the dynamics of motion and reflection of temperature solitons in wave heat transfer in limited regions. *Journal of Engineering Physics and Thermophysics*, vol. 93, no. 1, 10-15.
25. Formalev, V.F., Kolesnik, S.A., Kuznetsova, E.L. (2019). Approximate analytical solution of the problem of conjugate heat transfer between the boundary layer and the anisotropic strip. *Periodico Tche Quimica*, vol. 16, no. 32, 572-582.
26. Buktukov, N.S., Buktukov, B.Z., Moldabayeva, G.Z. (2020). Sail-aerodynamic wind power station with automatically changing blade-swept area. *International Journal of Mechanical and Production Engineering Research and Development*, vol. 10, no. 3, 911-920.
27. Kolesnik, S.A., Bulychev, N.A., Rabinskiy, L.N., Kazaryan, M.A. (2019). Mathematical modeling and experimental studies of thermal protection of composite materials under high-intensity effects of laser radiation. *Proceedings of SPIE – The International Society for Optical Engineering*, vol. 3, article number 113221R.
28. Ryndin, V.V. (2019). Calculation of the nonequilibrium systems consisting of an aggregate of locally-equilibrium subsystems. *Periodico Tche Quimica*, vol. 16, no. 33, 289-303.
29. Mykhalevskiy, D.M., Kychak, V.M. (2019). Development of information models for increasing the evaluation efficiency of wireless channel parameters of 802.11 standard. *Latvian Journal of Physics and Technical Sciences*, vol. 56, no. 5, 22-32.
30. Sultanov, K.S., Khusanov, B.E., Rikhsieva, B.B. (2020). Longitudinal waves in a cylinder with active external friction in a limited area. *Journal of Physics: Conference Series*, vol. 1546, no. 012140.
31. Maleev, R.A., Zuev, S.M., Fironov, A.M., Volchkov, N.A., Skvortsov, A.A. (2019). The starting processes of a car engine using capacitive energy storages. *Periodico Tche Quimica*, vol. 16, no. 33, 877-888.
32. Dinzhos, R.V., Lysenkov, E.A., Fialko, N.M. (2015). Features of thermal conductivity of composites based on thermoplastic polymers and aluminum particles. *Journal of Nano- and Electronic Physics*, vol. 7, no. 3, 03022.

Paper submitted: 21.08.2020.

Paper accepted: 22.10.2020.

This is an open access article distributed under the CC BY 4.0 terms and conditions.